Inter-Research Science Publisher

Marine Ecology Progress Series
Volume 753:1–18

Published January 30, 2025
https://doi.org/10.3354/meps14767

Autumn and winter plankton composition and size structure in the North Sea

Gregor Börner[1,*], Romain Frelat[2], Anna Akimova[3], Cindy van Damme[4], Myron A. Peck[5], Marta Moyano[6,7]

[1]Institute of Marine Ecosystem and Fishery Science, University of Hamburg, Große Elbstraße 133, Hamburg 22767, Germany
[2]International Livestock Research Institute, Nairobi 00100, Kenya
[3]Thünen Institute of Sea Fisheries, Herwigstraße 31, Bremerhaven 27572, Germany
[4]Wageningen Marine Research, Haringkade 1, 1976 CP Ijmuiden, The Netherlands
[5]Royal Netherlands Institute for Sea Research (NIOZ), Department of Coastal Systems (COS), PO Box 59, 1790 AB Den Burg (Texel), The Netherlands
[6]Norwegian Institute for Water Research (NIVA), Økernveien 94, 0579 Oslo, Norway
[7]Center for Coastal Research, University of Agder, Universitetsveien 25, 4604 Kristiansand, Norway

ABSTRACT: Plankton dynamics in temperate ecosystems have mainly been studied during productive seasons, with comparatively less research conducted during the winter, particularly on microplankton. We implemented plankton sampling during a regular fishery cruise to investigate North Sea micro- and mesozooplankton community composition, abundance, and size structure (55–2000 µm) during autumn (Buchan/Banks area) and winter (Downs area) between 2013 and 2019. Samples were analyzed using image-based techniques. Community diversity (broad taxa) was relatively similar across years in both areas, with diatoms and tripos taxa sets dominating the microplankton community and gastropods and copepods dominating the mesozooplankton group. The average micro- to mesozooplankton ratio (in abundance) was 90:1 for Buchan/Banks, resulting in an average (±SD) normalized abundance size spectra (NASS) slope of −1.45 ± 0.18. For Downs, the micro- to mesozooplankton ratio was 235:1 with a steeper NASS slope of −1.67 ± 0.20 due to fewer large organisms. Interannual changes in the planktonic community for each area and their potential environmental drivers were examined using redundancy analysis (including taxonomy and size) and correlation analysis using NASS slopes (size only). Both approaches highlighted the importance of water mass properties (e.g. salinity, temperature, turbidity) in shaping plankton dynamics, although the amount of explained variance differed between approaches (11 vs. 46%). Our results contribute to a better understanding of standing stocks of plankton and their environmental drivers. Specifically, novel insights were gained into microplankton dynamics, which play an important role in supporting the growth and survival of winter-spawned fish larvae in the North Sea.

KEY WORDS: Plankton dynamics · Microplankton · Mesozooplankton · Size spectra · Image-based analysis · FlowCAM · ZooSCAN

1. INTRODUCTION

Plankton is the foundation of the marine food webs, supporting the productivity of all higher trophic levels (Ryther 1969); thus, climate-related changes in plankton communities can result in cascading effects on the entire ecosystem (e.g. Sguotti et al. 2022). In temperate marine ecosystems, a considerable amount of research has focused on exploring changes in plankton phenology, abundance, and community

*Corresponding author: g.boerner88@gmail.com

Publisher: Inter-Research · www.int-res.com

composition during the productive season (i.e. spring bloom) due to its importance to key life cycle events for higher trophic levels (e.g. Capuzzo et al. 2018). By contrast, the low-productivity season (i.e. winter) has been comparatively poorly studied (e.g. Nohe et al. 2020). This is particularly the case for microzooplankton, including both protists (ciliates and dinoflagellates) and small metazoans (e.g. copepod nauplii, meroplanktonic larvae) between 20 and 200 µm in size. This small size fraction of plankton plays a significant role in the ecosystem as key consumers of primary production, as important players in the microbial loop, and as a potential prey source for mesozooplankton and fish larvae (e.g. Calbet 2008, Montagnes et al. 2010). During periods of low light intensity and nutrient limitation, the trophodynamic importance of protists and other microbial loop components can be enhanced (Fileman et al. 2011). Thus, monitoring of plankton dynamics during fall and winter is important to understand the dynamics of temperate marine ecosystems during times of low productivity.

The majority of broad-scale zooplankton monitoring programs worldwide focus on mesozooplankton (the size fraction between 200 and 2000 µm) (e.g. Richardson et al. 2006). For example, the Continuous Plankton Recorder (CPR) provides large-scale coverage on the abundance (semi-quantitative) and distribution of zooplankton (>270 µm) in surface waters year-round (Richardson et al. 2006, Dippner & Krause 2013). In contrast, microplankton (the size-fraction 20–200 µm) is mainly sampled either at fixed monitoring stations (e.g. Eloire et al. 2010) or during sporadic cruises, mainly for understanding processes that occur during productive seasons (e.g. Dolan et al. 2021, Yang et al. 2021). The reason behind the lack of long-term, large-scale microplankton data collection is likely due to logistical challenges in sampling (i.e. size range between water samples and regular plankton nets) and sample preservation (i.e. Lugol-preserved samples have a shelf life of 6–12 mo; Gifford & Caron 2000, Calbet et al. 2001). Implementing recent methods (e.g. image analysis, metabarcoding) to track changes in the composition and abundance of the entire planktonic community is now the goal of many monitoring programs embracing ecosystem-based management (Lombard et al. 2019, Garcia-Vazquez et al. 2021). Automatic processing of plankton samples using image analysis technologies and machine-learning algorithms is one of the cost-efficient alternatives to traditional time-consuming and costly microscopy (Goodwin et al. 2022, Irisson et al. 2022). These methods allow the processing of a larger number of samples, albeit at a lower taxonomic resolution than microscopy currently allows (i.e. rarely to species level). The outcomes of these methods (e.g. Flow Cytometer and Microscope [FlowCAM] or ZooSCAN) in terms of abundance, biomass, and seasonal variability of phyto- and zooplankton have been reported to compare well with traditional microscope counts, especially for the most abundant classes (e.g. Álvarez et al. 2014).

Given the functional complexity of the zooplankton community and the methodological difficulties involved with estimating its diversity, alternative metrics have been developed. A size-spectra approach, introduced by Sheldon et al. (1972), is a widely used approach to investigate the spatiotemporal variability of zooplankton, predator–prey interactions (e.g. Huebert & Peck 2014, Akimova et al. 2023), and to model the productivity of the higher trophic levels feeding on zooplankton (e.g. Blanchard et al. 2017, Serra-Pompei et al. 2022). The zooplankton size spectra is often reported in terms of the normalized abundance size spectra (NASS) or normalized biomass size spectra (NBSS) (Sprules & Barth 2016). The slope of NASS is believed to reflect the efficiency of the energy flux between trophic levels, whereas its intercept reflects the productivity of a given ecosystem (Zhou 2006, Ye et al. 2013).

The North Sea is a temperate shelf ecosystem with pronounced seasonal changes in primary and secondary productivity (Krause et al. 2003). The variability in oceanographic conditions and ecosystem processes is mainly linked to the North Atlantic influence at its open northern and southern boundaries, terrestrial influences along its shores, and Baltic Sea outflow in the east. Many components of the North Sea ecosystem have been measured extensively over the past decades. In terms of plankton, weekly time series spanning several decades are available for phyto-, micro-, and zooplankton at some fixed stations, such as Plymouth L4 (e.g. Eloire et al. 2010) or Helgoland Roads (e.g. Pitois et al. 2009). Additionally, CPR time series with a broader spatial scale are available for mesozooplankton groups, such as copepods, euphausiids, and meroplankton (e.g. Richardson et al. 2006, Dippner & Krause 2013). These time-series have revealed a number of regime shifts in the North Sea; the most recent one was associated with a decline in primary productivity and holoplankton, a northward shift in the distribution of cold-water copepod species such as *Calanus finmarchicus*, and an increased presence of small-sized, warm-water copepod species like *C. helgolandicus* (e.g. Capuzzo et al. 2018, Sguotti et al. 2022). However, as with other temperate ecosys-

tems, comparatively less is known about the microzooplankton community and its recent changes in the North Sea. Such information is relevant to provide a better understanding of the dynamics of lower trophic levels but also to shed light on prey fields available to higher trophic levels, such as early life stages of commercially important winter-spawning fishes like Atlantic herring *Clupea harengus* (Alvarez-Fernandez et al. 2015, Akimova et al. 2023). This knowledge is particularly relevant to exploring potential food limitations for fish early stages, which has been suggested as a potential driver (together with warming) of the relatively low recruitment success that has occurred in North Sea herring during the most recent decade (Alvarez-Fernandez et al. 2015 and references therein).

In this study, we investigated the North Sea micro- and mesozooplankton community during autumn and winter between 2013 and 2019 using image-based analysis (FlowCAM and ZooSCAN). Samples were obtained during a routine fisheries survey, which covered the traditional spawning grounds of Atlantic herring in the western (Buchan and Banks in September, autumn) and southern North Sea (Downs in late December, winter). Our objectives were to (1) describe plankton community composition and abundance in both sampling areas, (2) describe plankton size structure and size spectra metrics (NASS slopes and intercepts) for both sampling areas, and (3) identify spatial and interannual trends in the plankton community for each sampling site and link them to environmental variables using either diversity (i.e. broad taxonomic groups and size) or size composition only (NASS). Our results provide essential information on the standing stock of plankton in the 2 observed areas and its environmental drivers during the low-productivity season in the North Sea. Moreover, this information constitutes a unique database of available prey fields for early life stages of autumn- and winter-spawning fish in the areas. We discuss the benefits and drawbacks of the sampling methods and statistical approaches, as well as provide recommendations for future zooplankton monitoring in the North Sea and other temperate coastal systems.

2. MATERIALS AND METHODS

2.1. Sample collection

The plankton samples were taken on board the Dutch research vessel 'Tridens' within the framework of the International Herring Larval Survey (IHLS), coordinated by the International Council for the Exploration of the Sea. The Dutch surveys cover the 3 spawning grounds of the North Sea autumn-spawning herring: the Buchan and Banks region (hereafter Buchan/Banks) in September and Downs in late December (Fig. 1). At each station, ichthyo- and mesozooplankton were sampled using a modified GULF VII net (280 µm mesh size; Nash et al. 1998), which included a PUP-net (55 µm mesh size) for microplankton sampling (Fig. 2). This gear was towed in double oblique hauls at 5 knots down to 5 m above the sea floor to sample the whole water column. Although the pressure conditions differed between the 2 nets due to their different mesh sizes, the difference in cone openings (200 vs. 40 mm) but similar length played a crucial role in decreasing the in-net pressure on the organisms. Once onboard, plankton

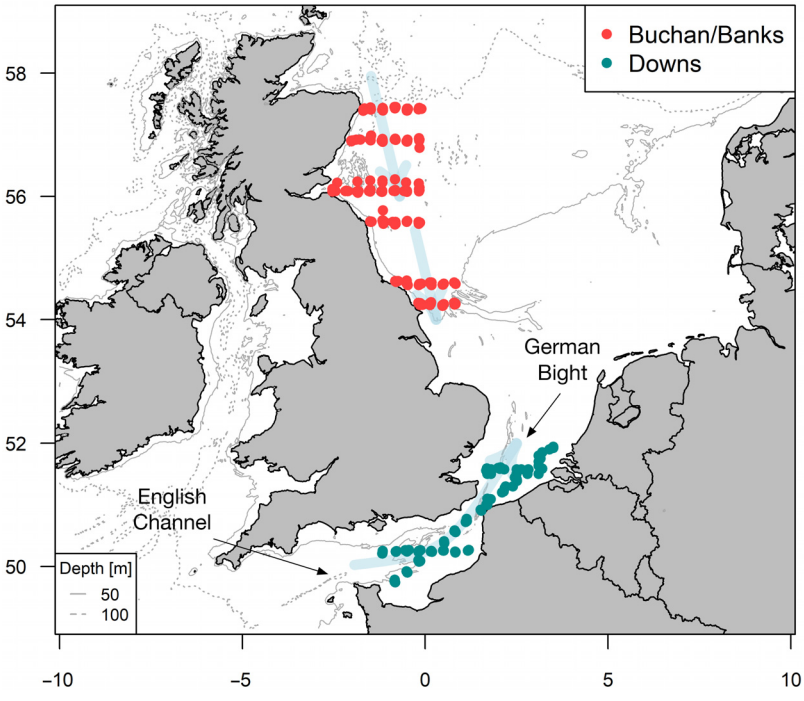

Fig. 1. Selected transects from the International Herring Larval Survey in the Buchan/Banks (September, autumn; red dots) and Downs spawning grounds (December, winter; cyan dots) analyzed in this study. Black arrows: the 2 subareas in the Downs spawning grounds (English Channel and Southern Bight); light arrows: path of the Atlantic water inflows through the English Channel and the northern boundary of the North Sea. See Fig. S1 for stations sampled each year

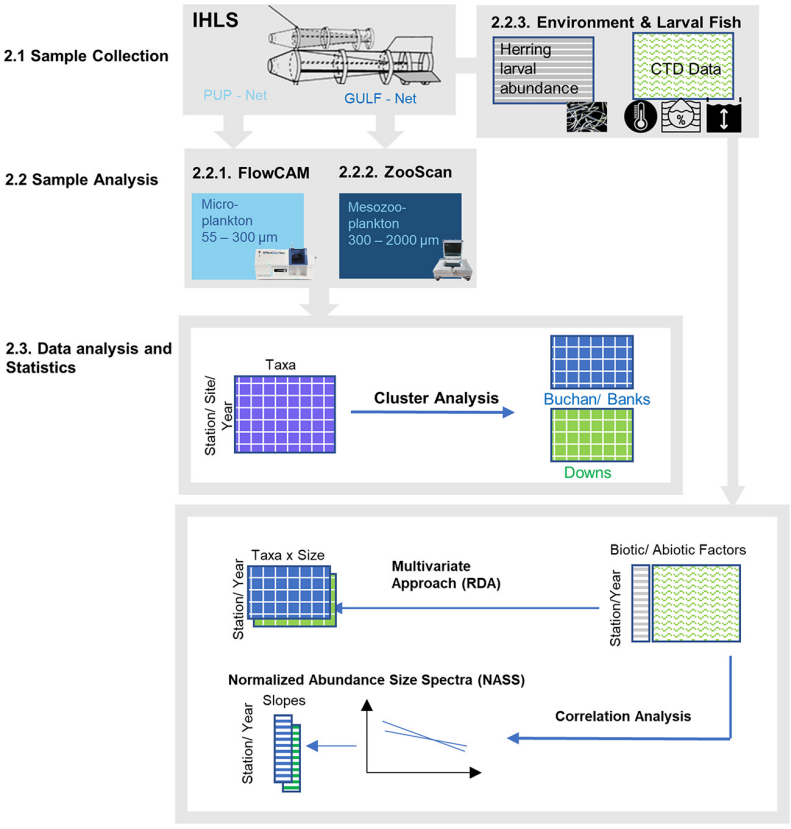

Fig. 2. Methodology for field sampling and data analyses. Numbers refer to section numbers

samples from both nets were preserved in 4% formaldehyde. Out of the sampling grid, 6 transects in Buchan/Banks and 3 transects in Downs were chosen for plankton analysis in this study (Fig. 1), representing the onshore–offshore and north–south gradients. Typically, 25–35 samples per season were analyzed, although in 3 Downs surveys, <10 samples were collected along the predefined transects (Fig. S1 in the Supplement at www.int-res.com/articles/suppl/m753p001_supp.pdf).

2.2. Sample analysis

2.2.1. Microplankton samples: FlowCAM

In the laboratory, the microplankton samples from the PUP net were rinsed and sieved through a 300 µm mesh. The fraction below 300 µm was retained and diluted (to approx. 4000 particles ml^{-1}; 50–500 ml, depending on the plankton concentration of the sample). Subsequently, the samples were analyzed using the FlowCAM (Yokagawa Fluid Imaging; Sieracki et al. 1998) with a 300 µm flow chamber (i.e. upper size limit for the particles analyzed). The amount of sample to process was set according to the particle concentration, aiming at approx. 10 000 pictures per sample containing a minimum of 10% living organisms (generally >30%). Subsequently, images were classified using the dynamic optimization cycle workflow principle described by Conradt et al. (2022), which involves an automated updating of the training data set based on manual-validation results to streamline the model adaptation process. Pictures of living organisms were grouped into 11 taxa sets: bivalves, tripos, ciliates, copepods, diatoms, dinoflagellates, dinophysis, foraminiferans, gastropods, protoperidinium, and silicoflagellates, which included species, genus, or families, with class as the lowest taxonomic resolution (Fig. S2). Note that the metazoan groups from the PUP net samples (bivalves, gastropods, and copepods) refer to their larval stages (e.g. nauplii in the case of copepods). The groups tripos, dinophysis, and protoperidinium correspond to dinophysids-, protoperidiniacean-, and triposids-dinoflagellates, respectively, but due to the distinct differences in shapes, these genus-sets were considered separately from the general dinoflagellate class (and are therefore referred to as 'tripos', 'dinophysis', and 'protoperidinium' throughout this article). Appendicularians from the PUP net samples were excluded from the analysis due to size measurement issues related to their transparency. Likewise, pictures of unknown organisms and non-living particles (such as detritus, sand, fibers, etc.) were excluded from further analysis. Note that the relative amount of detritus within each sample was calculated per station and used as an index of turbidity (in %).

2.2.2. Mesozooplankton samples: ZooSCAN

Mesozooplankton samples were subsampled using $1/16^{th}$ to $1/1024^{th}$ of the original sample following Motoda (1967), and one subsample per station was placed into ZooSCAN (v.2) (Gorsky et al. 2010). The images captured by ZooSCAN were classified automatically using ImageJ software (v.1.41o; https://imagej.net/ij/) with ZooProcess (v.7.19; Jalabert et al. 2024) and the Plankton Identifier software (v.1.3.4;

http://www.obs-vlfr.fr/~gaspari/Plankton_Identifier/index.php). The Plankton Identifier library was created in-house with images from the IHLS surveys and other North Sea cruises, and with about 200–300 vignettes per group as proposed by Gorsky et al. (2010). The automatic classification was followed by a final manual validation step. Organisms were grouped into 10 taxa sets: appendicularians, chaetognathans, cladocerans, copepods, diatoms, echinoderms, gastropods, jellies, malacostracans, and polychaetes (Fig. S2). The metazoan groups echinoderms, malacostracans, and gastropods refer to their larval stages. For microplankton, we treated classes that were easily distinguishable due to their shape as separate taxa sets. For instance, we pooled all gelatinous zooplankton except chaetognathans and appendicularians into the jellies taxa (mainly ctenophores). To ensure accurate size measurements across various taxonomic groups, we compared the measured sizes with values directly reported in the literature (e.g. Beaulieu et al. 1999, Dudeck et al. 2021) and with calculated metrics such as biovolume (BV) and carbon content (e.g. Kiørboe 2013, Menden-Deuer et al. 2001, Lehette & Hernández-León 2009). During manual validation, any multiples or clumps were removed, as their contribution to the total number of living organisms was less than 5%.

2.2.3. Environmental data and larval fish

Environmental variables (water temperature and salinity) were recorded by a CTD profiler (Seabird SBE 911) attached to the Gulf VII net. For further analysis, temperature and salinity were averaged over the upper 20 m of the water column. Turbidity was calculated based on the amount of detritus contained in each sample (see Section 2.2.1). Herring larvae in the GULF VII net were counted and measured to the nearest 1 mm. The larval number in each size class was then transformed into the larval abundance (ind. m^{-2}), using the volume of water filtered by the GULF net and the observed depth. Further technical and methodological details regarding larval handling and the survey can be found in Schmidt et al. (2009) and references therein.

2.2.4. Data analysis and statistics

Micro- and mesozooplankton data sets were combined for each sampling area to analyze the planktonic community between 55 and 2000 µm. Classes that were present in samples from both methods (copepods, gastropods, and diatoms) were merged together (Fig. S2). To avoid overlapping in size classes and double counts, taxa images in which the object size (equivalent spherical diameter) was <300 µm were excluded from the mesozooplankton data set.

The BV (μm^3) of each planktonic organism was calculated using a modified version of the formula proposed by Saccà (2016):

$$\mathrm{BV}\,(\mu m^3) = \frac{4}{3} \times \sqrt{\pi^{-1} \times \mathrm{AR} \times A^3} \quad (1)$$

where AR is the aspect ratio (ratio between the width and the length of individual organisms) and A is the area (μm^2) of each organism. Both values were determined using FlowCAM and ZooSCAN. The BV was then used to calculate the carbon biomass for the different plankton taxa using taxa-specific equations (Table S1) (Menden-Deuer et al. 2001, Kiørboe 2013). Note that sizes (width and length) were not corrected by the potential effect of fixation. We are aware that fixation can cause swelling, shrinking, or even the loss of certain organisms (e.g. Calbet & Saiz 2005), and we discuss this topic below (see Section 4.1).

The number of organisms counted per sample and per taxa set was recalculated in plankton concentration (ind. m^{-3}) using information about the volume of water sampled by a net and the dilutional factor described above. Although the plankton concentration was used in the statistical analyses below, we followed the common terminology in the plankton literature (Sprules & Barth 2016) and refer to it as 'abundance', meaning the abundance of the observed organisms in one cubic meter.

Hierarchical cluster analysis (HCA) was applied to detect changes in the plankton community across seasons and areas. To assess normality, the Anderson-Darling test (Nelson 1998) was performed on the abundance data, which indicated a significant deviation from normality (A = 3940.1, $p < 0.001$). As a result, the data was scaled using the triple-square-root transformation to reduce skewness (Legendre & Gallagher 2001) and ensure that the assumptions for the subsequent analyses were met. After transformation, the Euclidean distance was calculated, and the Ward linkage was applied to the abundance data per species of the taxonomic groups and surveys (Buttigieg & Ramette 2014, Murtagh & Legendre 2014). To investigate the changes in plankton size structure, NASS were constructed for each station. Slopes based on abundance (i.e. NASS) rather than biomass or BV were selected due to the higher adjusted R^2 of the linear fit to the normalized abundance data in compari-

son to biomass or BV and the fact that NASS relied only on the size parameters directly measured with FlowCAM and ZooSCAN (Fig. S3). All zooplankton organisms were grouped into size classes based on their BV (irrespective of taxa), using a doubling or octave scale (Sheldon et al. 1972, Blanco et al. 1994). Size classes with low counts (0.01% of all records) were excluded, leading to classes ranging between size 14 (BV ~1.6×10^5 µm^3) and 33 (BV ~8.5×10^9 µm^3). The total abundance of each size class was divided by its width (in terms of BV) to normalize the size spectra. A linear weighted regression was fit to these data:

$$\log_2\beta(\mathrm{BV}) = a \log_2(\mathrm{BV}) + b \quad (2)$$

where a and b are the slope and the intercept of the NASS β (BV), respectively. Weights of the regression were proportional to the zooplankton abundance in the corresponding BV classes.

The influence of environmental drivers on the plankton community was explored using 2 approaches: a correlation analysis on the size-resolved data set (NASS slopes) and a redundancy analysis (RDA) which used the taxa- and size-resolved plankton community structure (Legendre 2001). The RDA was selected because an initial detrended correspondence analysis of the species abundance indicated that the length of the first axis was short (1.4 SD), suggesting that linear ordination techniques were most appropriate (Lepš & Šmilauer 2003). We assessed variance homogeneity for the RDA using Levene's test. Initially, significant variance differences across groups were detected (F = 18.391, p < 0.001). However, following the Hellinger transformation (Legendre & Gallagher 2001), the test indicated no significant variance differences (F = 0.4976, p = 1.0), satisfying the assumption of homoscedasticity required for further analysis. For each sampling area, an RDA was performed on a matrix of the transformed abundance of size classes × taxa sets in columns and hauls (or stations) in rows.

Therefore, we understand the variability in the planktonic community as the among-station variations in concentrations of the different taxa sets within different size classes.

The environmental variables used in the RDA and correlation analysis included water temperature and salinity averaged over the upper 20 m, distance to shore (m), depth (m), and turbidity (%). We chose to average temperature and salinity over the upper 20 m as the majority of plankton biomass is concentrated in the upper mixed layer (Mikaelyan et al. 2021). We repeated the analyses using depth-averaged temperature and salinity, and the results were similar to those using the average of the upper 20 m (data not shown). Moreover, we used the larval herring abundance (ind. m^{-2}) for each station as an additional explanatory variable. In the size-based approach, Pearson correlation (Pearson 1896) was used to identify the relations between the potential environmental drivers and NASS slopes. The significance of the RDA results was assessed for both the complete RDA and for each RDA axis using the marginal method (Legendre et al. 2011) with the 'anova.cca' function in the 'vegan' R package (Oksanen et al. 2022), employing 999 permutations. We applied the 'pcaiv' function in the 'ade4' package (Dray & Dufour 2007) for the RDAs, as it is optimal for visualization of the fitted scores on the constrained RDA axes. The significance of each explanatory variable on the principle components (RDA-PCs) was additionally tested using the 'ANOVA' test in the 'ade4' package.

All analyses and graphical representations were performed using the R software (R Core Team 2022). The RDA was performed using the 'ade4' package (Bougeard & Dray 2018) and the HCA was performed with the 'gplots' package (Warnes et al. 2022). All data sets and corresponding code can be accessed through the Zenodo repository (Boerner et al. 2024).

3. RESULTS

3.1. Plankton community composition

In total, 18 taxonomic groups of plankton were identified across both areas. Most taxa were present in all surveys, except 2 Downs surveys in 2013 and 2018 with reduced spatial coverage (Fig. 3, Fig. S4, Tables S2 & S3). The HCA clearly separated the planktonic communities in Buchan/Banks and Downs (Fig. 3). Tripos, diatoms, dinophysis, silicoflagellates, ciliates, protoperidinium, and gastropod larvae showed the highest abundances in Buchan/Banks (>5% contribution to the total abundance; Table S2). Diatoms and copepod nauplii dominated the planktonic community in Downs in terms of abundance (>4% relative contribution; Table S3).

Overall, microplankton taxa (including copepod nauplii) contributed >98% to the total plankton abundance, of which diatoms and tripos dominated (>50% in Buchan/Banks and 90% in Downs) (Tables S2 & S3). Copepod nauplii were less abundant (approx. 4–5% of the total microplankton abundance; Tables S2 & S3) but they dominated in terms of biomass (27% of the total microplankton biomass in Buchan/Banks vs. 41% in Downs; Tables S4 & S5). For the mesozoo-

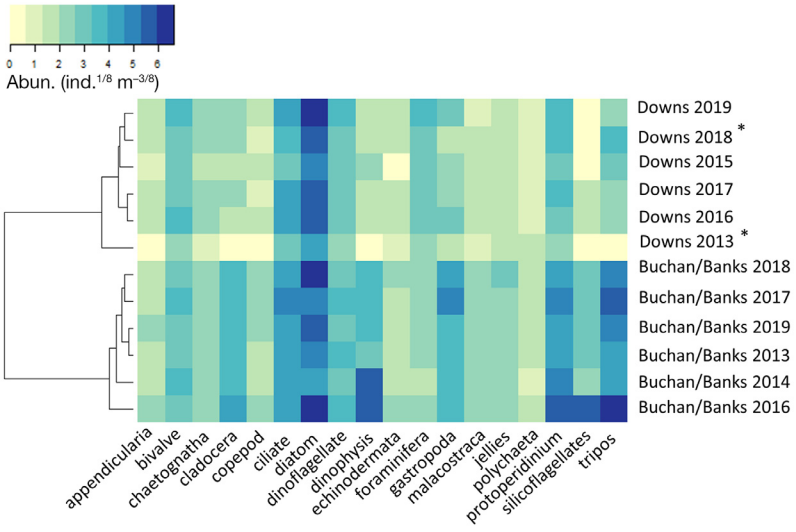

Fig. 3. Clustering and associated heatmap of the abundance of different micro- and mesozooplankton taxa (*x*-axis) for each of the analyzed North Sea cruises (*y*-axis indicates location [Downs or Buchan/Banks] and year). Colors indicate the strength of association by showing the frequency of triple-square-root transformed abundance (ind.$^{1/8}$ m^{-3}) per taxa in each year and area. The dendrogram clusters together cruises from each area. Asterisks indicate years with reduced spatial coverage (see Fig. S1)

plankton, gastropods and larger copepods dominated the community in both areas in terms of both abundance and biomass, contributing on average 10% (30%) of total mesozooplankton abundance and 38% (43%) of total biomass in Buchan/Banks (Downs). The average abundance ratio of microplankton to mesozooplankton was 90:1 for Buchan/Banks and 235:1 for Downs (Tables S3 & S4).

3.2. Environmental drivers of plankton abundance and distribution

Environmental conditions were distinct and showed clear spatial patterns in both studied areas and seasons. We provide more details on the environmental conditions in Fig. S5 and focus here only on their relations with the planktonic community.

In the Buchan/Banks area, the 6 explanatory variables used in the RDA explained 11.4% of the variation in plankton community composition, whereby half of this variation (6%) was summarized in the first principal component (RDA-PC1) (Fig. 4A). Although the total explained variance was relatively low, this component was deemed significant following the conducted statistical test. Therefore, in what follows we focus only on the leading RDA-PC1. Medium-sized gastropods, ciliates, and chaetognathans (size classes 18–22) had the highest positive scores in RDA-PC1, while small silicoflagellates, dinophysis, and jellies (size class 14–17) had the highest negative scores (Fig. 4A,B). Larger size classes (26–33) did not show any pattern and their RDA-PC1 scores ranged between −0.1 and 0.1 (Fig. 4B). The observed spatial pattern in the Buchan/Banks area (Fig. 4C) was consistent over the sampled years, except for 2016, which exhibited negative scores at most stations (Fig. 4D). These negative scores were likely influenced by the higher contribution of silicoflagellates, dinophysis, and jellies, which could be attributed to the exceptionally low salinity observed in the entire Buchan/Banks region in 2016. All 6 explanatory variables were significant (ANOVA, $p < 0.05$); specifically, depth ($F_{1,189} = 42.96$, $p < 0.001$), salinity ($F_{1,189} = 1320.00$, $p < 0.001$), turbidity ($F_{1,189} = 141.70$, $p < 0.001$), temperature ($F_{1,189} = 6.12$, $p = 0.014$), distance ($F_{1,189} = 18.26$, $p < 0.001$), and herring larvae ($F_{1,189} = 5.85$, $p = 0.017$). Salinity, turbidity, and depth had the highest positive scores, mainly in northern stations (Fig. 4C,E). Note that the RDA repeated based on BV (rather than on abundance) reported similar spatial patterns and relationships with the environmental variables (Fig. S6).

In the Downs area, the RDA explained 10.6% of the variability in plankton community composition of which 33.5% (3.6% of total variation) was explained by the first principal component (RDA-PC1; Fig. 5A). Similarly, to the Buchan/Banks area, this component was found to be significant. Large chaetognathans (size class 30–31), tripos, and dinoflagellates were more abundant in the English Channel, while medium- to large-sized copepods (size class 26–28), polychaetes, and jellies were more prevalent in the Southern Bight stations and had the highest positive scores (Fig. 5A,B). Most of the distribution of scores per size class crossed zero (except classes 14, 15, 19, and 22), and the absolute value of the median score per size class was between −0.2 and 0.2; hence, there was no pronounced effect of most size classes on RDA-PC1 (Fig. 5B). The described west–east pattern was detected in all years with full spatial coverage (2016, 2017, and 2019) (Fig. 5C,D). Four of the 6 explanatory variables (temperature, salinity, depth, and turbidity) had a significant effect on RDA-PC1 (Fig. 5E). Specifically, depth (ANOVA, $F_{1,89} = 97.14$, $p < 0.001$), temperature (ANOVA, $F_{1,89} = 342.50$, $p < 0.001$), salinity (ANOVA,

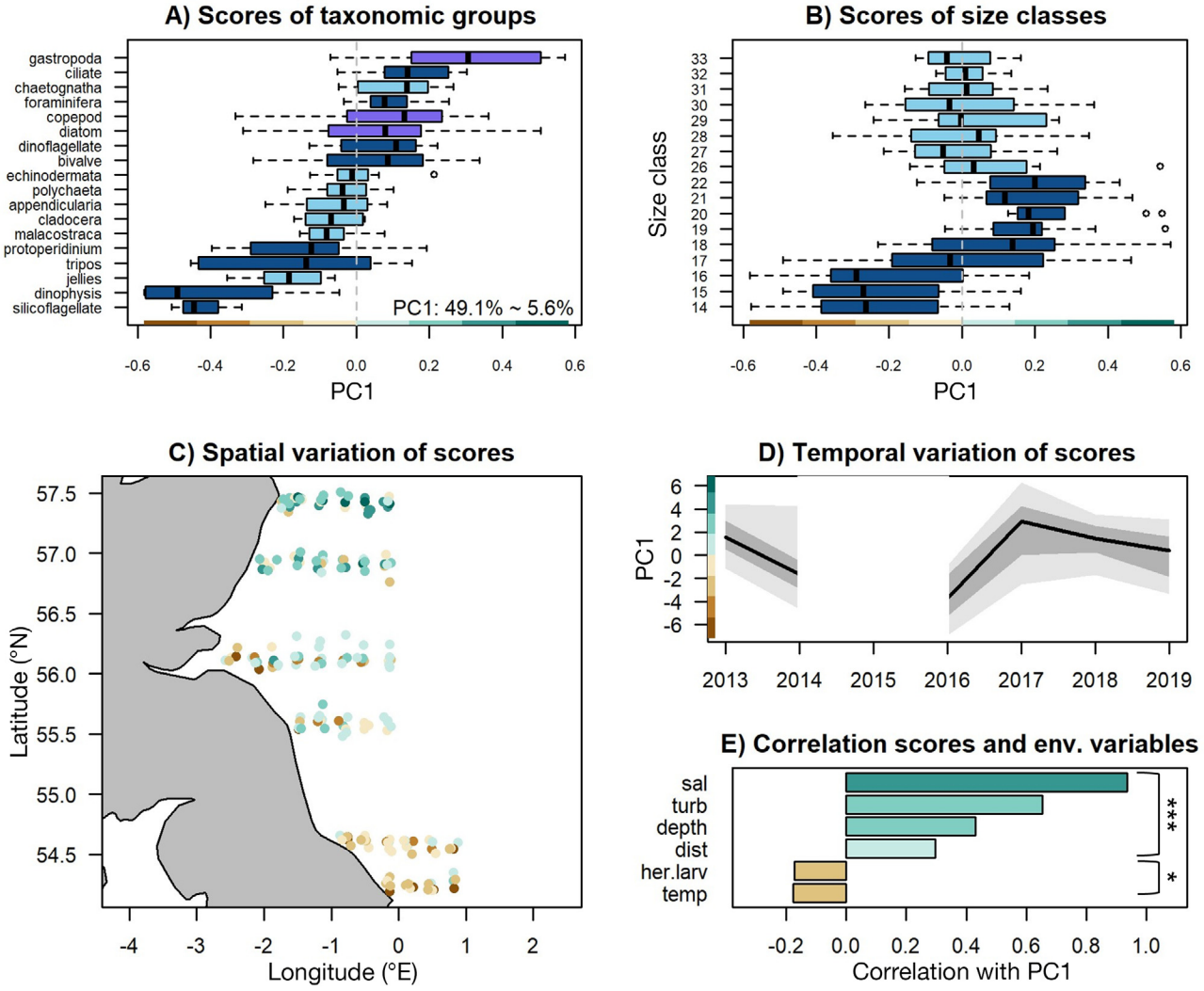

Fig. 4. Redundancy analysis (RDA) examining the effect of 5 environmental drivers (distance to shore [dist], turbidity [turb], salinity [sal], temperature [temp], and bottom depth [depth]) and herring larvae abundance (her.larv) on the zooplankton community composition and distribution during the Buchan/Banks surveys (September, autumn). Scores of the (A) Principal Component 1 (PC1) among taxonomic groups and the explained variability and (B) size classes, with the different types indicated in dark blue (FlowCAM), light blue (ZooSCAN), and purple (both). (C) Station scores and spatial variation; station coordinates are jittered to avoid overlap among years. (D) Temporal variation of station scores. Bold black line: median; dark grey shading: interquartile range; light grey shading: 95% quantiles. (E) Pearson correlation coefficient between the PC1 and the 6 explanatory variables. Color intensity is proportional to the correlation coefficients (brown: negative; cyan: positive) and shows the impact on the respective station. Asterisks indicate significance: *p < 0.05; ***p < 0.001

$F_{1,89}$ = 69.06, p < 0.001), and turbidity (ANOVA, $F_{1,89}$ = 16.17, p = 0.0001) were significant. Overall, temperature, salinity, and depth had the highest negative scores. Stations with negative scores were generally located in the deeper, southwestern part of the Downs area and were associated with higher temperature and higher salinity than the northeastern stations (Fig. 5E). Similarly, to the Buchan/Banks area, the RDA repeated based on BV (rather than on abundance) resulted in similar spatial patterns and relationships with the environmental variables (Fig. S7).

Larval herring abundance, used as a predation index, had a significant effect on the RDA-PC1 in Buchan/Banks (ANOVA, $F_{1,189}$ = 5.849, p = 0.017) and Downs (ANOVA, $F_{1,89}$ = 4.074, p = 0.047). However, the score of herring larvae consistently exhibited values close to zero, suggesting a minimal effect on larval predation on the plankton community (Pearson's correlation coefficient, r > −0.2). These correlation coefficients were similar when the analysis was repeated only with suitable prey items of herring larval foraging as described in Akimova et al. (2023) (Fig. S8).

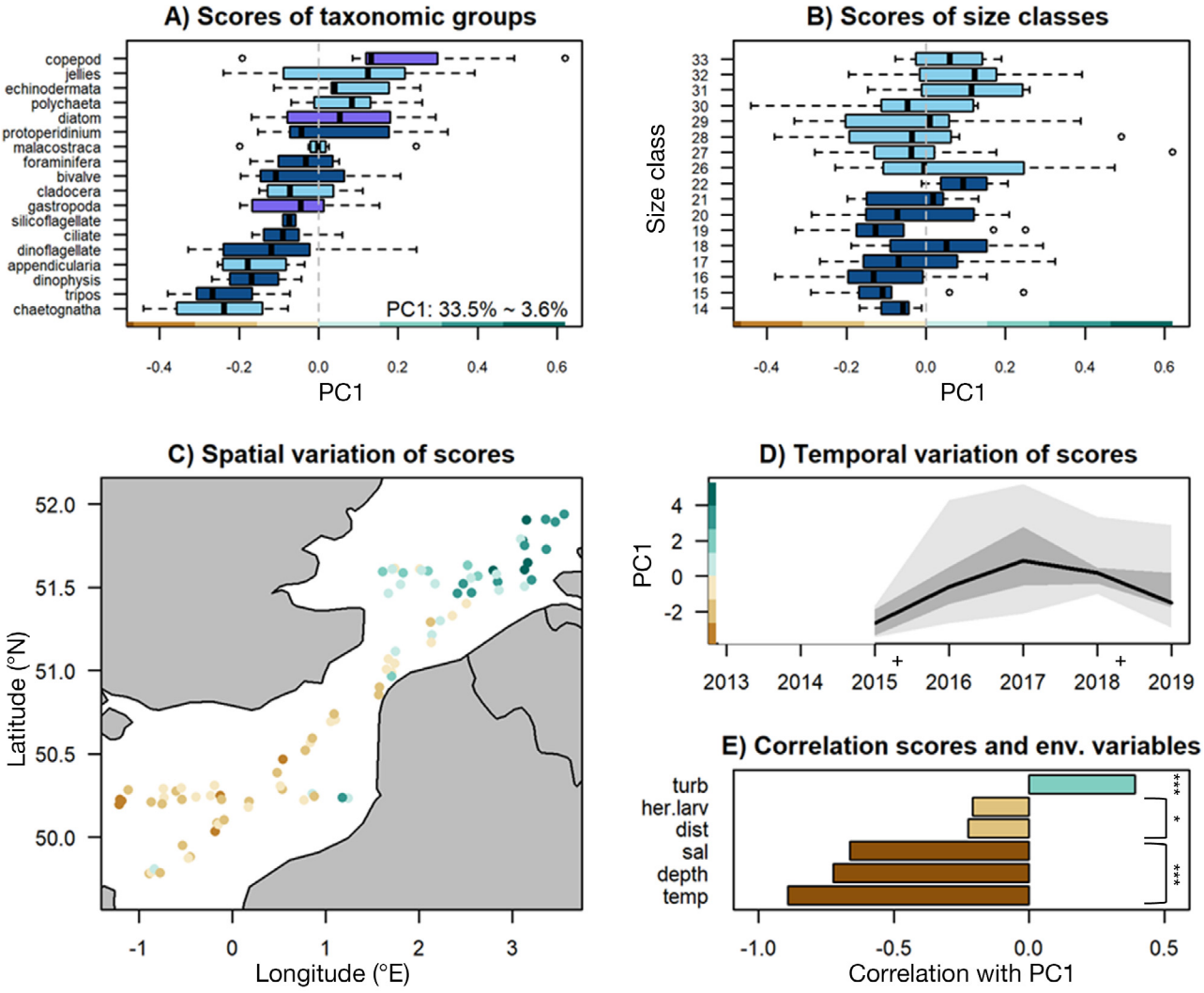

Fig. 5. Same as Fig. 4, but for the Downs surveys (December, winter). In (D), $^{+}$ indicates incomplete sampling. Asterisks indicate significance: *p < 0.05; ***p < 0.001

3.3. Plankton size structure and environmental drivers

The total mean NASS slope for Buchan/Banks was −1.45 (Fig. 6A), with most frequent values ranging between −1.2 and −1.6 (Fig. 6B). Linear fits for the NASS slopes had the adjusted R^2 ranging between 0.86 and 0.98, typically >0.95 (Fig. S9). NASS was positively correlated with turbidity and salinity and negatively correlated with temperature (Fig. 6E), indicating a tendency towards flatter slopes (i.e. a higher relative abundance of larger organisms) at stations with higher turbidity and salinity and lower temperature. Mean NASS slope was steeper in 2014 and 2016 (<−1.6) than in 2017, 2018, and 2019 (>−1.4) (Fig. 6D). Similarly, these 2 years (2014 and 2016) showed slightly distinct spatial patterns as the north−south spatial gradient in the slopes was not apparent (Fig. S10). The NASS slopes in Buchan/Banks showed the strongest correlations with salinity and turbidity (r = 0.57 and 0.58, respectively, p < 0.001), but correlations with all other environmental variables except herring larval abundance were found to be significant at p < 0.05 as well (Fig. 6E).

In Downs, the mean NASS slope was −1.67 (Fig. 7A), with the highest frequencies between −1.9 and −1.6 (Fig. 7B). The NASS slopes in Downs showed a spatial gradient with flatter size spectra (>−1.4) in the northeastern stations and steeper slopes (<−1.6) in the southwestern stations (Fig. 7C,D). This pattern was present in all years with full spatial coverage (2016, 2017, 2019) (Fig. S11). The NASS slopes in this area showed a high negative correlation with temperature, salinity, and depth (r = −0.52, −0.49, and −0.34,

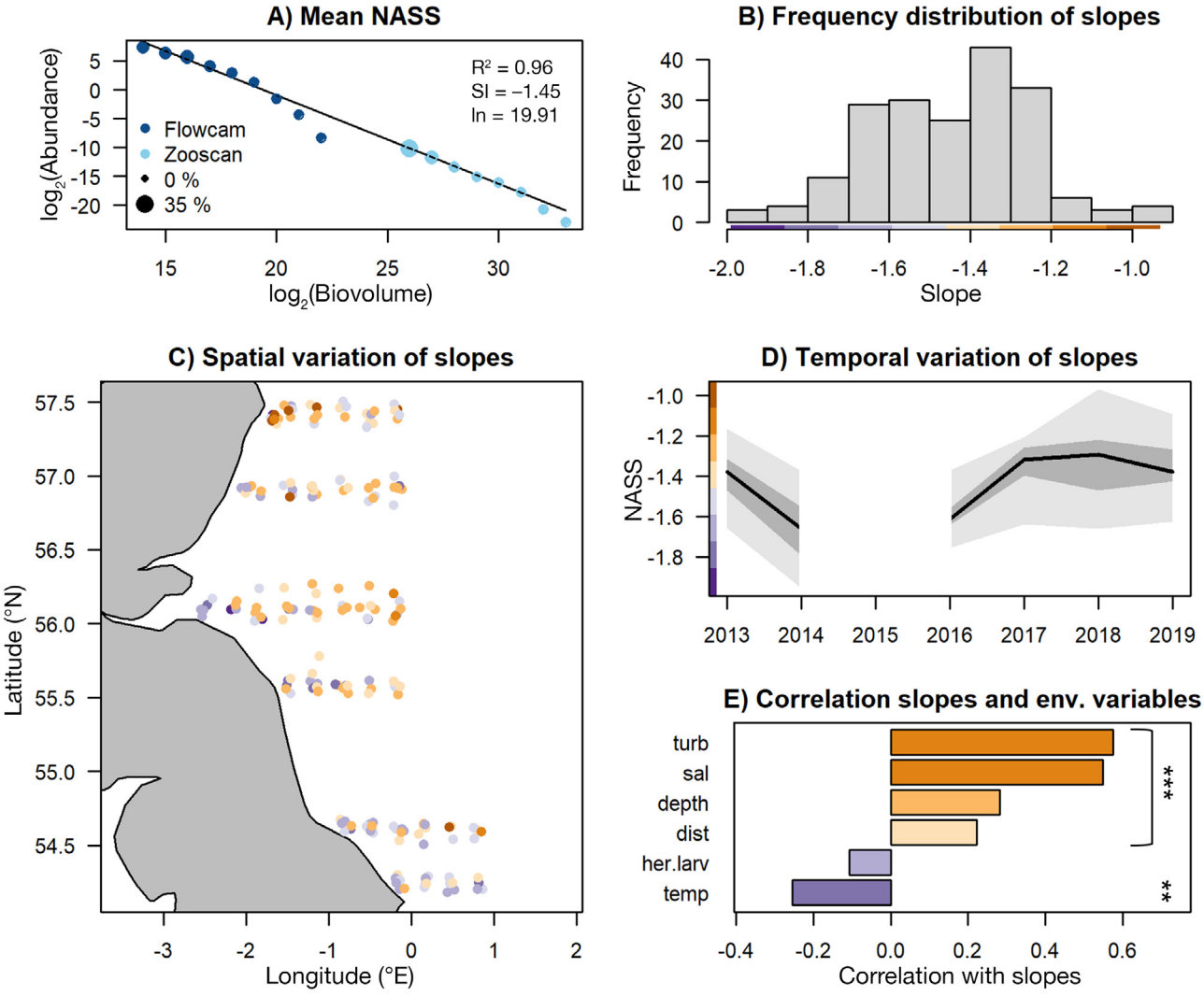

Fig. 6. (A) Mean normalized abundance size spectra (NASS) calculated for all stations in the Buchan/Banks survey in September (autumn). Dot sizes represent the relative abundance of the size class used in the weighted linear regression to derive the slope of the size spectra. R^2: goodness of fit; Sl: slope; In: intercept. (B) Histogram showing the distribution of individual slopes. (C) NASS slope depicted in colors showing its spatial variation; station coordinates are jittered to avoid overlap. (D) Temporal variation of the NASS slope. Bold black line: median; dark grey area: interquartile range; light grey area: 95% quantiles. (E) Pearson correlation coefficient between the slope and the 6 explanatory variables (see Fig. 4 for abbreviations). Color intensity is proportional to the correlation coefficients (purple: negative; orange: positive). Asterisks indicate significance: **$p < 0.01$; ***$p < 0.001$

respectively, $p < 0.001$) (Fig. 7E), while turbidity showed the highest positive correlation ($r = 0.58$, $p < 0.001$) (Fig. 7E).

4. DISCUSSION

4.1. Community composition in Buchan/Banks and Downs areas

The present study provides broad-scale information about the standing stocks of micro- and mesozooplankton in the western North Sea (autumn) and the southern North Sea (winter) over 7 consecutive years. The planktonic community was found to be homogeneous in terms of the relative contribution of the different broad taxonomic groups across years in each sampling area and season. Generally, the observed broad range in mesozooplankton abundance was consistent with other studies in these areas (Table S6). For example, the mean abundance of copepod nauplii in autumn and winter (55 and 38.1 ind. l^{-1}, respectively) was similar to values reported at the Dove station (4.0–20.0 ind. l^{-1} in autumn, 15.0–43.0 ind. l^{-1} in

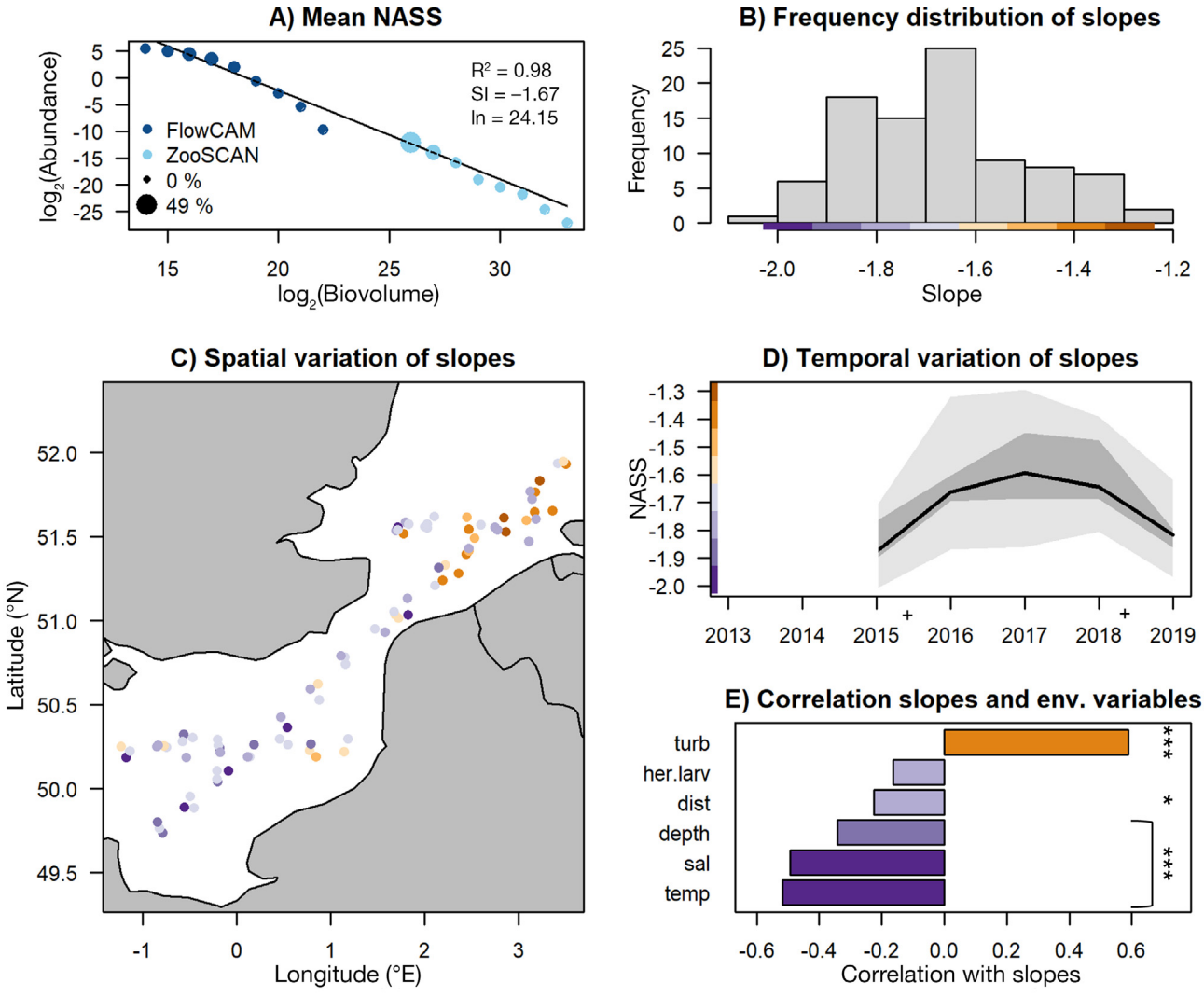

Fig. 7. Same as Fig. 6, but for the Downs survey in December (winter). In (D), $^{+}$ indicates incomplete sampling. Asterisks indicate significance: *p < 0.05; ***p < 0.001

winter; Pitois et al. 2009). However, note that the average mesozooplankton abundance tended to be slightly higher in coastal monitoring stations (e.g. L4, Dove station) compared to cruises with larger spatial coverage (as in this study). For example, the observed total plankton abundance in the English Channel during winter was within the range of previously reported values (354.9 vs. 266.6 ind. m^{-3} in Dudeck et al. 2021), but slightly lower than winter averages in the L4 station (1500.0 ind. m^{-3} in Eloire et al. 2010) (Table S6).

Additionally, the observed low plankton abundance in particular years (see e.g. 2013 and 2019; Table S3) could have also contributed to those slightly lower overall abundances. The relative abundance of various groups such as copepods (60–80%) agrees well with other studies (e.g. Morse et al. 2017; Table S6).

The sampling method presented here, using 2 plankton nets simultaneously (mesh sizes 55 and 280 µm), has already been proposed as the most adequate approach to capture the entire mesozooplankton assemblage, including small copepods (e.g. *Oithona* spp.) and other small metazoans (Calbet et al. 2001). In this study, on average, 11% more of the copepodites and adult copepods (>200 µm) were captured in the 55 µm plankton net compared to the 280 µm GULF VII alone. The abundance of mesozooplankton caught in the GULF net alone was 7.2 times lower when using only a traditional 280 µm net versus a combination with a 55 µm net, similar to a previous study (8.1 times lower; Calbet et al. 2001). This finding advocates for the combined use of different mesh-sized nets in large-scale routine monitoring programs to gain a more realistic estimate of large

microzooplankton and the entire mesozooplankton community.

The mean abundance of protists (dinoflagellates and ciliates) obtained in this study within each sampling area was between 2 and 6 orders of magnitude lower than previously reported for the North Sea (Bresnan et al. 2015, Bils et al. 2019; Table S6). The difference in findings can be attributed to variations in sampling and preservation approaches employed. Previous studies utilized Niskin bottles for sampling and preserved the samples in Lugol, whereas in the current study, a PUP net was used for sampling and the samples were fixed with formaldehyde. Mesh filtering of plankton nets can result in up to a 60% reduction in protist abundance (Gifford & Caron 2000), which here may be further intensified by damage from clogging or the drag induced by the small mesh size. Additionally, the use of formaldehyde fixation can result in the dissolution of soft-bodied dinoflagellates and ciliates (Calbet & Saiz 2005). Therefore, it is important to interpret our results for protozoa with caution, as our method may underestimate their abundance. Among the ciliates, tintinnids are the only group able to better withstand various types of preservation and filtration (Modigh & Castaldo 2005). For this group, the abundances reported here were comparable with a previous study in the North Sea (Bils et al. 2019; Table S6).

4.2. Plankton size structure in Buchan/Banks and Downs areas

Body size is an important ecological trait that is relatively easy to measure in plankton samples, especially via automatic image analysis, and these body sizes can be used to build zooplankton size spectra (either NASS or NBSS), which can serve as indicators of ecosystem status (Blanchard et al. 2017, Atkinson et al. 2021) and are helpful tools for identifying alterations in the food-web structure (Gorokhova et al. 2016). Zooplankton size spectra has been widely used as an alternative metric to analyze the structure and the dynamics of marine ecosystems without having to address their species composition (Blanco et al. 1994, Zhou 2006). Following Atkinson et al. (2021), we argue in our study that sampling plankton abundance over a broad size range is essential for obtaining a reliable estimate of the size spectra. Utilizing partial size spectra (e.g. exclusively micro- or mesoplankton data) can introduce either a positive or negative bias into derived size-spectrum slopes (as demonstrated in Fig. S12). However, caveats are required with respect to the limitations of each individual sampling method. In our study, the employed method likely underestimated the abundance of microplankton organisms due to formalin preservation and net selectivity, as mentioned above. This can potentially lead to steeper NASS slopes than those reported here. Unfortunately, we are not aware of any prior study reporting the magnitude of such underestimation in microplankton abundance.

The NASS slopes reported in our study appear shallower than the theoretical value of −2.0 (Blanco et al. 1994). However, making a direct comparison of our findings with previous studies is challenging due to variations in variables, units, and axis scaling within size-spectra approaches (Blanco et al. 1994, Sprules & Barth 2016). Additionally, the plankton size spectrum can be influenced by sampling, counting, and preservation methodologies (Álvarez et al. 2014). Due to these methodological differences, only a comparison of spatial and temporal variability in slopes is feasible here. Clear variations in the slope have been previously demonstrated across inshore and offshore areas or across seasons (Zhang et al. 2019). For instance, steeper slopes were observed offshore for nano- and microplankton in the South China Sea (Liu et al. 2021), whereas slopes of mesoplankton size spectra were found to decrease from nearshore to offshore in the subarctic North Pacific (Kwong et al. 2022). Seasonal variations, with steeper slopes during the winter, have been reported in temperate seas (Atkinson et al. 2021). These findings are consistent with the steeper slopes observed in winter in Downs (mean ± SD: −1.67 ± 0.18) in comparison to those observed in autumn in Buchan/Banks (−1.45 ± 0.20). NASS intercepts were similar in both sampling areas and seasons, although Buchan/Banks in autumn had a wider range in intercepts (5–30) compared to Downs in winter (15–30). If we consider the intercept as a reflection of the primary production (Ye et al. 2013), production levels were comparable across the different seasons and areas.

4.3. Spatial gradients and environmental drivers of the plankton taxonomic composition and size structure in Buchan/Banks

Among the environmental factors tested here, salinity, turbidity, depth, and distance to the coast were found to be the main drivers of the plankton community and size composition in Buchan/Banks in autumn (Figs. 4E & 6E). Temperature and salinity are

known to be related to the water masses and their dynamics, whereas turbidity (defined here as percentage of detritus) is mainly driven by processes such as river runoff, dust deposition, and resuspension of seabed sediments. No clear temperature gradient was observed between these 2 water masses during our sampling in autumn (Fig. S3), and temperature explained only a small part of the variance in both RDA ($r = -0.17$) and correlation analysis ($r = -0.25$) applied to the zooplankton data in this region (Figs. 4E & 6E).

The studied area is strongly influenced by the inflow of highly saline Atlantic water and river runoff (Lee 1980). The Atlantic water flows southward and mixes gradually with the less saline North Sea coastal waters influenced by freshwater discharge from the Tyne, Tees, and Humber rivers (Emeis et al. 2015). Previous research has highlighted the impacts of water mass dynamics and Atlantic inflow on the planktonic community's variability in the North Sea (e.g. Krause et al. 2003, Taylor et al. 2021).

In our study, gastropod larvae and chaetognaths were found in higher abundances at the northern stations of Buchan/Banks, in an area strongly influenced by the Atlantic inflow. This agrees with previous findings of the gastropods *Spiratella retroversa*, *Clione limancina*, and the chaetognath *Sagitta elegans* being characteristic taxa in the northwestern North Sea (Vane 1961, Bone et al. 1987). Tintinnids (the major group in the ciliate taxa set in this study) were found to be abundant at the northern stations in Buchan/Banks as well, whereas they have previously been reported to be more abundant in the southern North Sea during wintertime (Bils et al. 2019). This discrepancy may be related to the different environmental preferences of different tintinnid species (e.g. salinity; Cordeiro et al. 1997), which were not accounted for in our broad taxa sets. Silicoflagellates, dinoflagellates (such as *Dinophysis* spp.), and gelatinous plankton (pooled as 'jellies' here) were more abundant in the fresher and shallower waters in the south. Although nutrients were not measured, we speculate that those taxa sets were more abundant there due to an elevated nutrient concentration associated with the river runoff as suggested by Jochem & Babenerd (1989) and Purcell et al. (2001). Turbidity was identified as another factor significantly related to the variability of the zooplankton community and its size structure. However, turbidity in this area was positively correlated to salinity and, therefore, high turbidity cannot be ascribed to the river inflow there. Further investigations will be required to understand the source of the elevated turbidity in the northern part of the Buchan/Banks area associated with the Atlantic Water Inflow.

The percentage of variance in the plankton community explained by the RDA with environmental constraints was relatively low (11.4% in Buchan/Banks and 10.6% in Downs). While the leading RDA-PC1 component was deemed significant in both areas, the overall findings should be approached with caution, as they accounted only for a small portion of the variation in the taxonomical and size structure of plankton (6% in Buchan/Banks and 3.6% in Downs). Potential explanations for this are discussed in Section 4.5.

Changes in the NASS slope in Buchan/Banks were consistent with the observed community composition and the distribution of the water masses, and a similar north–south gradient was apparent. Turbidity and salinity were also the environmental variables with a higher correlation ($r > 0.55$). NASS slopes did not show a clear north–south gradient in 2014 and 2016, years that had steeper average slopes (<-1.6) compared to the others. The reasons behind these differences remain unclear. For 2016, this may be related to the exceptionally low salinity registered across the whole sampling area. This was probably linked to a relatively low salinity of the Atlantic Water Inflow in the North Sea, caused by a strong Subpolar Gyre phase (Taylor et al. 2021).

The abundance of herring larvae had a weak effect in the RDA-PC1 ($r > -0.2$) and appeared as a non-significant effect in the correlation analysis ($r < -0.1$). This is in line with other studies that also observed no significant effects of larval predation on zooplankton biomass in the Newfoundland coastal waters (Pepin & Penney 2000). Our approach of combining planktonic organisms into broad taxonomic groups did not allow an elaboration of the complex food-web dynamics within the zooplankton community, but it provided relevant data sets for exploring larval fish feeding in the area. Using the present zooplankton data set, a recent work explored potential food limitation in both sampling areas by employing an individual-based model of larval herring foraging and growth (Akimova et al. 2023). This study by Akimova et al. (2023) suggested that the amount of available zooplankton and its size composition was adequate to support the survival of elder herring larvae (>11 mm), whereas it severely limited growth and survival of the first-feeding larvae smaller than 8 mm. The model results suggested that first-feeding larvae were at a larger risk of starvation (74% of the stations for 8 mm larvae) in Buchan/Banks, but that this risk decreased to 5–10% of the stations for larvae >11 mm. For larvae >15 mm, more than half of the stations supported ad libitum

larval growth. Their results contribute to increase our understanding of the role of starvation mortality in the recruitment success of autumn-spawning North Sea herring.

4.4. Spatial gradients and environmental drivers of the plankton taxonomic composition and size structure in Downs

The Downs region during winter consistently encountered a prominent southwest–northeast gradient from warmer, more saline and less turbid waters of Atlantic origin flowing through the English Channel to colder, fresher and more turbid coastal waters in the Southern Bight (Fig. S3). Chaetognaths, dinoflagellates, and tripos were dominant taxa in the central English Channel, whereas large copepods, jellies, and echinoderm larvae were more abundant in the Southern Bight. These results agree with the reported higher winter abundance of copepods near the Belgium and Dutch coasts compared to the English Channel (Dudeck et al. 2021). Although small gelatinous organisms are generally known to thrive in warmer waters, high abundances of these organisms have been previously observed during colder months across the North Sea and in the Celtic Sea (Purcell 2005, Haberlin et al. 2019). Similar to the Buchan and Banks area, we presume that a nutrient flux from the Rhine-Meuse-Scheldt delta can potentially explain the elevated jellyfish abundance in the Southern Bight (Purcell et al. 2001). Furthermore, the river discharge seems to cause the observed elevated turbidity in low saline waters in the Southern Bight.

Turbidity was found to be positively correlated with the NASS slope. This suggests that elevated turbidity was associated with a higher relative abundance of larger size classes, like mesozooplankton, while smaller categories (microplankton) may display a contrasting reaction, similar to trends observed in estuarine settings such as Chesapeake Bay (Roman et al. 2001, Keller et al. 2014). Turbidity seems to also influence the extent of diel vertical migrations in copepods, which has been reported to be size-dependent (Ohman & Romagnan 2016). The latter study suggested that increased light attenuation may reduce diel vertical migrations of medium-sized copepods, which are the ones exhibiting larger vertical migrations compared to small- and large-sized copepods. Given the increased turbidity and darkening projected for the North Sea (Capuzzo et al. 2018 and references therein), it is important to continue exploring how the distribution and behavior of different zooplankton organisms change in response to the different climate change factors (and their interactions).

Similar to the Buchan/Banks area, herring larval predation was not significantly correlated with zooplankton community and size structure in Downs. Results from the above-mentioned individual-based model for larval herring from Akimova et al. (2023) showed that herring larvae between 6 and 26 mm in length experienced substantial starvation in these areas in winter, albeit starvation mortality was higher in smaller larvae (>80%) than in larger ones (ca. 35%). As the authors highlighted in that study, it is difficult to reconcile the high starvation potential with current trends in the autumn-spawning North Sea herring population, where the contribution of the Downs component is increasing. Therefore, further investigation of the interplay between larval starvation and predation is required in the future. Simultaneous sampling of zooplankton and herring larvae during the IHLS as performed here is helpful to assess realistic larval foraging success and separate integrated larval mortality into its starvation and predation components.

4.5. Taxonomic information versus size spectra

Plankton time-series are increasingly used to inform policy and management about the state and productivity of marine ecosystems (Bedford et al. 2018, 2020b). In particular, fisheries management is interested in zooplankton data, given that fish early life stages and recruitment success often depend on zooplankton stock and productivity (Garrido et al. 2024). In this regard, it is important to generate data at an adequate spatial and temporal resolution that can reveal changes in ecosystem functioning under variable environmental conditions (Scott et al. 2023). The development of easy and time- and cost-effective tools to provide key data on plankton groups and their abundance or biomass is thus gaining increased attention (e.g. Pollina et al. 2022). The state-of-the-art automated image processing, although time-effective, currently allows the identification of zooplankton organisms to rather broad taxonomical groups (e.g. copepods, chaetognaths, dinoflagellates) and barely to the species level. However, such analysis seems to be adequate to provide the abundance and biomass of certain zooplankton groups, which have been used to detect large-scale, long-term changes in the planktonic community in response to climate-related processes (e.g. Bedford et

al. 2020a, Scott et al. 2023) or to assess prey availability to study foraging of fish larvae (Akimova et al. 2023). However, this broad taxonomical resolution precludes a thorough exploration of the environmental drivers affecting the community composition. For instance, the copepod taxa set was likely composed of a mixture of several species common in the North Sea (e.g. *Calanus finmarchicus*, *C. helgolandicus*, *Oithona atlantica*, and *O. similis*), each of them having a distinct affinity for temperature and salinity (Lindegren et al. 2020). In our study, the environmental variables accounted for a small proportion (ca. 11%) of the overall spatial and interannual variability of the planktonic community (see Section 3.5). The limited explanatory power of the environmental variables could be attributed to the general inherent variability associated with plankton sampling and the restricted scope of the environmental variables used, which did not include conditions preceding sampling. Internal biological interactions and small-scale dynamics may be responsible for a significant variance in the data sets that cannot be explained by environmental variability.

Using a size-spectra approach allows us to focus only on the size structure of the zooplankton community and reduces the amount of noise in the data stemming from such small-scale species interactions or limitations of the taxa identification methods. The environmental variables used in this study explained between 34 and 52% of the variability in the size-spectra slope in both areas (see Section 4.3). It is worth noting that the most important environmental drivers identified in the correlation analyses with NASS slope were consistent with those identified in the RDA using species- and size-resolved data. This points out the usefulness of the size-spectrum approach as a simplistic metric to describe ecosystem status and environmentally driven changes in food-web structure and ecosystem productivity (Sprules & Munawar 1986, Petchey & Belgrano 2010). Thorough explorations of the plankton community should encompass a broad range of organismal weights. Atkinson et al. (2021) suggested that data to construct a reliable size spectrum should cover at least 7 orders of magnitude to include small phytoplankton and zooplankton. In addition, spatial and temporal integration should be incorporated to avoid short-term snapshots that could be misleading.

The results from our study highlight the benefits and limitations of using taxonomically and size-resolved plankton data sets compared to solely size-resolved ones alone. The choice of a suitable methodology not only needs to consider the level of community and spatial resolution required to answer a particular research question but also practical aspects such as available effort and expertise. Ideally, both taxonomically and size-resolved approaches should be used in parallel to explore different aspects of the planktonic community.

4.6. Conclusions and outlook

The present study provides a thorough exploration of the plankton standing stocks and spatial—interannual changes in micro- and mesozooplankton abundance in the temperate North Sea during low productivity seasons. The planktonic community was shaped along environmental gradients, primarily salinity, temperature, and turbidity, which are related to inflows of North Atlantic waters in the western and southern North Sea. These gradients were apparent when analyzing the community structure as broad taxa and size spectrum slopes, suggesting that the latter can be useful to track environmentally driven changes in the plankton community.

Annual ichthyoplankton surveys, such as IHLS, offer a unique and low-cost opportunity for sampling micro- and mesozooplankton. Prior to implementing our sampling, the IHLS only quantified herring larvae captured in the Gulf VII samples and a few other planktonic organisms targeted for specific analyses (e.g. Dudeck et al. 2021). However, our annual sampling is an example of the way forward to more holistic sampling, which is needed to support an ecosystem-based approach to fisheries. The combination of survey instruments such as the PlanktoScope (Pollina et al. 2022) with automated plankton classification tools (Conradt et al. 2022) can greatly reduce the effort needed to process zooplankton samples, allowing for higher-frequency spatiotemporal sampling of lower trophic level organisms building the base of the marine food web. Ultimately, the combination of both traditional and novel instruments and procedures will help optimize survey designs (Scott et al. 2023) to obtain a more complete understanding of the processes involved. Zooplankton sampling simultaneously with regular scientific fishery surveys can substantially expand existing global, publicly accessible plankton data sets. These data sets can be used to better understand factors affecting ecosystem productivity and to develop early warning indicators for hydro-climatic changes in rapidly changing marine ecosystems (Bedford et al. 2018, Taylor et al. 2021). Furthermore, they can be used to validate nutrient—phytoplankton—

zooplankton–detritus models (D'Alelio et al. 2016) or build physiological models of fish larvae (Akimova et al. 2023).

Data availability. All data sets and corresponding code can be accessed through the Zenodo repository at https://doi.org/10.5281/zenodo.13616727.

Acknowledgements. This research was funded by the German Research Foundation (DFG) under project THRESHOLDS (Disentangling the effects of climate-driven processes on North Sea herring recruitment through physiological thresholds, MO 2873-3-1). We sincerely thank the crew, students, and cruise leaders of the IHLS onboard the RV 'Tridens', especially Ewout Blom and Marcel de Vries. Furthermore, we thank Rachel Harmer, Franziska Bils, and Silke Janßen for their support on cruises and plankton analysis, as well as Angela Olvera Pascual, Sophie Lanners, Svenja Heckler, and Julian Koplin, who helped to scan and sort the plankton pictures. We also thank Eva Alvarez for her support with the size-spectra approach, Saskia Otto and Jie Liu for statistical advice, and contributing editor Rebecca Asch and 4 anonymous reviewers who helped improve the manuscript. The present work was part of G.B.'s PhD thesis at the University of Hamburg.

LITERATURE CITED

Akimova A, Peck MA, Börner G, van Damme C, Moyano M (2023) Combining modeling with novel field observations yields new insights into wintertime food limitation of larval fish. Limnol Oceanogr 68:1865–1879

Álvarez E, Moyano M, López-Urrutia Á, Nogueira E, Scharek R (2014) Routine determination of plankton community composition and size structure: a comparison between FlowCAM and light microscopy. J Plankton Res 36: 170–184

Alvarez-Fernandez S, Licandro P, Van Damme CJG, Hufnagl M (2015) Effect of zooplankton on fish larval abundance and distribution: a long-term study on North Sea herring (*Clupea harengus*). ICES J Mar Sci 72:2569–2577

Atkinson A, Lilley MKS, Hirst AG, McEvoy AJ and others (2021) Increasing nutrient stress reduces the efficiency of energy transfer through planktonic size spectra. Limnol Oceanogr 66:422–437

Beaulieu SE, Mullin MM, Tang VT, Pyne SM, King AL, Twining BS (1999) Using an optical plankton counter to determine the size distributions of preserved zooplankton samples. J Plankton Res 21:1939–1956

Bedford J, Johns D, Greenstreet S, McQuatters-Gollop A (2018) Plankton as prevailing conditions: a surveillance role for plankton indicators within the Marine Strategy Framework Directive. Mar Policy 89:109–115

Bedford J, Johns DG, McQuatters-Gollop A (2020a) Implications of taxon-level variation in climate change response for interpreting plankton lifeform biodiversity indicators. ICES J Mar Sci 77:3006–3015

Bedford J, Ostle C, Johns DG, Atkinson A and others (2020b) Lifeform indicators reveal large-scale shifts in plankton across the North-West European shelf. Glob Change Biol 26:3482–3497

Bils F, Moyano M, Aberle N, van Damme CJG and others (2019) Broad-scale distribution of the winter protozooplankton community in the North Sea. J Sea Res 144: 112–121

Blanchard JL, Heneghan RF, Everett JD, Trebilco R, Richardson AJ (2017) From bacteria to whales: using functional size spectra to model marine ecosystems. Trends Ecol Evol 32:174–186

Blanco J, Echevarria F, Garcia CM (1994) Dealing with size-spectra: some conceptual and mathematical problems. Sci Mar 58:17–29

Boerner G, Frelat R, Akimova A, van Damme C, Peck MA, Moyano M (2024) Data from: autumn and winter plankton composition and size structure in the North Sea (data set). Zenodo, https://doi.org/10.5281/zenodo.13616727

Bone Q, Brownlee C, Bryan GW, Burt GR and others (1987) On the differences between the two 'indicator' species of chaetognath, *Sagitta setosa* and *S. elegans*. J Mar Biol Assoc UK 67:545–560

Bougeard S, Dray S (2018) Supervised multiblock analysis in R with the ade4 package. J Stat Softw 86:1–17

Bresnan E, Cook KB, Hughes SL, Hay SJ, Smith K, Walsham P, Webster L (2015) Seasonality of the plankton community at an east and west coast monitoring site in Scottish waters. J Sea Res 105:16–29

Buttigieg PL, Ramette A (2014) A guide to statistical analysis in microbial ecology: a community-focused, living review of multivariate data analyses. FEMS Microbiol Ecol 90: 543–550

Calbet A (2008) The trophic roles of microzooplankton in marine systems. ICES J Mar Sci 65:325–331

Calbet A, Saiz E (2005) The ciliate–copepod link in marine ecosystems. Aquat Microb Ecol 38:157–167

Calbet A, Garrido S, Saiz E, Alcaraz M, Duarte CM (2001) Annual zooplankton succession in coastal NW Mediterranean waters: the importance of the smaller size fractions. J Plankton Res 23:319–331

Capuzzo E, Lynam CP, Barry J, Stephens D and others (2018) A decline in primary production in the North Sea over 25 years, associated with reductions in zooplankton abundance and fish stock recruitment. Glob Change Biol 24:e352–e364

Conradt J, Börner G, López-Urrutia Á, Möllmann C, Moyano M (2022) Automated plankton classification with a dynamic optimization and adaptation cycle. Front Mar Sci 9:868420

Cordeiro TA, Brandini FP, Martens P (1997) Spatial distribution of the Tintinnina (Ciliophora, Protista) in the North Sea, spring of 1986. J Plankton Res 19:1371–1383

D'Alelio D, Libralato S, Wyatt T, Ribera D'Alcalà M (2016) Ecological-network models link diversity, structure and function in the plankton food-web. Sci Rep 6:21806

Dippner JW, Krause M (2013) Continuous Plankton Recorder underestimates zooplankton abundance. J Mar Syst 111–112:263–268

Dolan JR, Moon JK, Yang EJ (2021) Notes on the occurrence of tintinnid ciliates, and the nasselarian radiolarian *Amphimelissa setosa* of the marine microzooplankton, in the Chukchi Sea (Arctic Ocean) sampled each August from 2011 to 2020. Acta Protozool 60:1–11

Dray S, Dufour AB (2007) The ade4 package: implementing the duality diagram for ecologists. J Stat Softw 22:1–20

Dudeck T, Rohlf N, Möllmann C, Hufnagl M (2021) Winter zooplankton dynamics in the English Channel and southern North Sea: trends and drivers from 1991 to 2013. J Plankton Res 43:244–256

Eloire D, Somerfield PJ, Conway DVP, Halsband-Lenk C, Harris R, Bonnet D (2010) Temporal variability and community composition of zooplankton at station L4 in the Western Channel: 20 years of sampling. J Plankton Res 32:657–679

Emeis KC, van Beusekom J, Callies U, Ebinghaus R and others (2015) The North Sea — a shelf sea in the Anthropocene. J Mar Syst 141:18–33

Fileman ES, Fitzgeorge-Balfour T, Tarran GA, Harris RP (2011) Plankton community diversity from bacteria to copepods in bloom and non-bloom conditions in the Celtic Sea in spring. Estuar Coast Shelf Sci 93:403–414

Garcia-Vazquez E, Georges O, Fernandez S, Ardura A (2021) eDNA metabarcoding of small plankton samples to detect fish larvae and their preys from Atlantic and Pacific waters. Sci Rep 11:7224

Garrido S, Albo-Puigserver M, Moyano M (2024) Larval trophic ecology of small pelagic fishes: a review of recent advances and pathways to fill remaining knowledge gaps. Mar Ecol Prog Ser 741:127–143

Gifford DJ, Caron DA (2000) Sampling, preservation, enumeration and biomass of marine protozooplankton. ICES Zooplankton Methodol Man 2000:193–221

Goodwin M, Halvorsen KT, Jiao L, Knausgård KM and others (2022) Unlocking the potential of deep learning for marine ecology: overview, applications, and outlook. ICES J Mar Sci 79:319–336

Gorokhova E, Lehtiniemi M, Postel L, Rubene G and others (2016) Indicator properties of Baltic zooplankton for classification of environmental status within marine strategy framework directive. PLOS ONE 11:e0158326

Gorsky G, Ohman MD, Picheral M, Gasparini S and others (2010) Digital zooplankton image analysis using the ZooScan integrated system. J Plankton Res 32:285–303

Haberlin D, Raine R, McAllen R, Doyle TK (2019) Distinct gelatinous zooplankton communities across a dynamic shelf sea. Limnol Oceanogr 64:1802–1818

Huebert KB, Peck MA (2014) A day in the life of fish larvae: modeling foraging and growth using quirks. PLOS ONE 9:e98205

Irisson JO, Ayata SD, Lindsay DJ, Karp-Boss L, Stemmann L (2022) Machine learning for the study of plankton and marine snow from images. Annu Rev Mar Sci 14:277–301

Jalabert L, Elineau A, Brandão M, Picheral M (2024) Zooscan-Zooprocess user manual and procedures at the Quantitative Imaging Platform of Villefranche-sur-Mer (PIQv) (Version V3). Zenodo, https://doi.org/10.5281/zenodo.13949803

Jochem F, Babenerd B (1989) Naked *Dictyocha speculum* — a new type of phytoplankton bloom in the Western Baltic. Mar Biol 103:373–379

Keller DP, Lee DY, Hood RR (2014) Turbidity maximum entrapment of phytoplankton in the Chesapeake Bay. Estuar Coast 37:279–298

Kiørboe T (2013) Zooplankton body composition. Limnol Oceanogr 58:1843–1850

Krause M, Fock H, Greve W, Winkler G (2003) North Sea zooplankton: a review. Senckenb Marit 33:71–204

Kwong LE, Ross T, Lüskow F, Florko KRN, Pakhomov EA (2022) Spatial, seasonal, and climatic variability in mesozooplankton size spectra along a coastal-to-open ocean transect in the subarctic Northeast Pacific. Prog Oceanogr 201:102728

Lee AJ (1980) North Sea: physical oceanography. In: Banner FT, Collins MB, Massie KS (eds) The North-West European shelf seas: the sea bed and the sea in motion II. Physical and chemical oceanography, and physical resources. Elsevier Oceanography Series, Vol 24B. Elsevier, Amsterdam, p 467–493

Legendre P (2001) Model II regression user's guide. R Vignette 4:1–14. https://CRAN.R-project.org/web/packages/lmodel2/vignettes/mod2user.pdf

Legendre P, Gallagher ED (2001) Ecologically meaningful transformations for ordination of species data. Oecologia 129:271–280

Legendre P, Oksanen J, ter Braak CJF (2011) Testing the significance of canonical axes in redundancy analysis. Methods Ecol Evol 2:269–277

Lehette P, Hernández-León S (2009) Zooplankton biomass estimation from digitized images: a comparison between subtropical and Antarctic organisms. Limnol Oceanogr Methods 7:304–308

Lepš J, Šmilauer P (2003) Multivariate analysis of ecological data using CANOCO. Cambridge University Press, https://doi.org/10.1017/CBO9780511615146

Lindegren M, Thomas MK, Jónasdóttir SH, Nielsen TG, Munk P (2020) Environmental niche separation promotes coexistence among ecologically similar zooplankton species — North Sea copepods as a case study. Limnol Oceanogr 65:545–556

Liu Z, Li QP, Ge Z, Shuai Y (2021) Variability of plankton size distribution and controlling factors across a coastal frontal zone. Prog Oceanogr 197:102665

Lombard F, Boss E, Waite AM, Uitz J and others (2019) Globally consistent quantitative observations of planktonic ecosystems. Front Mar Sci 6:196

Menden-Deuer S, Lessard EJ, Satterberg J (2001) Effect of preservation on dinoflagellate and diatom cell volume and consequences for carbon biomass predictions. Mar Ecol Prog Ser 222:41–50

Mikaelyan AS, Pautova LA, Fedorov AV (2021) Seasonal evolution of deep phytoplankton assemblages in the Black Sea. J Sea Res 178:102125

Modigh M, Castaldo S (2005) Effects of fixatives on ciliates as related to cell size. J Plankton Res 27:845–849

Montagnes DJS, Dower JF, Figueiredo GM (2010) The protozooplankton–ichthyoplankton trophic link: an overlooked aspect of aquatic food webs. J Eukaryot Microbiol 57:223–228

Morse RE, Friedland KD, Tommasi D, Stock C, Nye J (2017) Distinct zooplankton regime shift patterns across ecoregions of the US Northeast continental shelf Large Marine Ecosystem. J Mar Syst 165:77–91

Motoda S (1967) Devices of simple plankton apparatus III. Bull Fac Fish Hokkaido Univ 18:3–8

Murtagh F, Legendre P (2014) Ward's hierarchical agglomerative clustering method: Which algorithms implement Ward's criterion? J Classif 31:274–295

Nash RDM, Dickey-Collas M, Milligan SP (1998) Descriptions of the Gulf VII/PRO-NET and MAFF/Guildline unencased high-speed plankton samplers. J Plankton Res 20:1915–1926

Nelson LS (1998) The Anderson-Darling test for normality. J Qual Technol 30:298–299

Nohe A, Goffin A, Tyberghein L, Lagring R, De Cauwer K, Vyverman W, Sabbe K (2020) Marked changes in diatom and dinoflagellate biomass, composition and seasonality in the Belgian Part of the North Sea between the 1970s and 2000s. Sci Total Environ 716:136316

Ohman MD, Romagnan J (2016) Nonlinear effects of body

size and optical attenuation on diel vertical migration by zooplankton. Limnol Oceanogr 61:765–770
Oksanen J, Simpson G, Blanchet F, Kindt R and others (2022) vegan: community ecology package. R package version 2.6-4. https://CRAN.R-project.org/package=vegan
Pearson K (1896) VII. Mathematical contributions to the theory of evolution. — III. Regression, heredity, and panmixia. Philos Trans R Soc Lond A Contain Pap Math Phys Character 187:253–318
Pepin P, Penney R (2000) Feeding by a larval fish community: impact on zooplankton. Mar Ecol Prog Ser 204: 199–212
Petchey OL, Belgrano A (2010) Body-size distributions and size-spectra: universal indicators of ecological status? Biol Lett 6:434–437
Pitois SG, Shaw M, Fox CJ, Frid CLJ (2009) A new fine-mesh zooplankton time series from the Dove sampling station (North Sea). J Plankton Res 31:337–343
Pollina T, Larson AG, Lombard F, Li H and others (2022) PlanktoScope: affordable modular quantitative imaging platform for citizen oceanography. Front Mar Sci 9: 949428
Purcell JE (2005) Climate effects on formation of jellyfish and ctenophore blooms: a review. J Mar Biol Assoc UK 85:461–476
Purcell JE, Breitburg DL, Decker MB, Graham WM, Youngbluth MJ, Raskoff KA (2001) Pelagic cnidarians and ctenophores in low dissolved oxygen environments: a review. In: Rabalais NN, Turner RE (eds) Coastal hypoxia: consequences for living resources and ecosystems. Coastal and Estuarine Studies, Vol 58. American Geophysical Union, Washington, DC, p 77–100
R Core Team (2022) R: a language and environment for statistical computing. R Foundation for Statistical Computing, Vienna
Richardson AJ, Walne AW, John AWG, Jonas TD and others (2006) Using Continuous Plankton Recorder data. Prog Oceanogr 68:27–74
Roman MR, Holliday DV, Sanford LP (2001) Temporal and spatial patterns of zooplankton in the Chesapeake Bay turbidity maximum. Mar Ecol Prog Ser 213:215–227
Ryther JH (1969) Photosynthesis and fish production in the sea. Science 166:72–76
Saccà A (2016) A simple yet accurate method for the estimation of the biovolume of planktonic microorganisms. PLOS ONE 11:e0151955
Schmidt JO, Van Damme CJG, Röckmann C, Dickey-Collas M (2009) Recolonisation of spawning grounds in a recovering fish stock: recent changes in North Sea herring. Sci Mar 73:153–157
Scott J, Pitois S, Creach V, Malin G, Culverhouse P, Tilbury J (2023) Resolution changes relationships: optimizing sampling design using small scale zooplankton data. Prog Oceanogr 210:102946
Serra-Pompei C, Ward BA, Pinti J, Visser AW, Kiørboe T, Andersen KH (2022) Linking plankton size spectra and community composition to carbon export and its efficiency. Global Biogeochem Cycles 36:e2021GB007275
Sguotti C, Blöcker AM, Färber L, Blanz B and others (2022) Irreversibility of regime shifts in the North Sea. Front Mar Sci 9:945204
Sheldon RW, Prakash A, Sutcliffe WH (1972) The size distribution of particles in the ocean. Limnol Oceanogr 17: 327–340
Sieracki CK, Sieracki ME, Yentsch CS (1998) An imaging-in-flow system for automated analysis of marine microplankton. Mar Ecol Prog Ser 168:285–296
Sprules WG, Barth LE (2016) Surfing the biomass size spectrum: some remarks on history, theory, and application. Can J Fish Aquat Sci 73:477–495
Sprules WG, Munawar M (1986) Plankton size spectra in relation to ecosystem productivity, size, and perturbation. Can J Fish Aquat Sci 43:1789–1794
Taylor MH, Akimova A, Bracher A, Kempf A, Kühn B, Hélaouët P (2021) Using dynamic ocean color provinces to elucidate drivers of North Sea hydrography and ecology. J Geophys Res Oceans 126:e2021JC017686
Vane FR (1961) Continuous plankton records: contribution to a plankton atlas of the NE Atlantic and the North Sea. Part VI: the seasonal and annual distribution of the Gastropoda. Bull Mar Ecol 5:247–253
Warnes G, Bolker B, Bonebakker L, Gentleman R and others (2022) gplots: various R programming, tools for plotting data. R package version 3.1.3. https://CRAN.R-project.org/web/packages/gplots/index.html
Yang J, Chen Z, Chen D, Xu D (2021) Spatial distribution of the microzooplankton communities in the northern South China Sea: insights into their function in microbial food webs. Mar Pollut Bull 162:111898
Ye L, Chang CY, García-Comas C, Gong GC, Hsieh CH (2013) Increasing zooplankton size diversity enhances the strength of top-down control on phytoplankton through diet niche partitioning. J Anim Ecol 82:1052–1061
Zhang W, Sun X, Zheng S, Zhu M, Liang J, Du J, Yang C (2019) Plankton abundance, biovolume, and normalized biovolume size spectra in the northern slope of the South China Sea in autumn 2014 and summer 2015. Deep Sea Res II 167:79–92
Zhou M (2006) What determines the slope of a plankton biomass spectrum? J Plankton Res 28:437–448

Editorial responsibility: Rebecca G. Asch, Greenville, North Carolina, USA
Reviewed by: J. Irisson and 3 anonymous referees
Submitted: August 8, 2023; Accepted: December 2, 2024
Proofs received from author(s): January 21, 2025